Ground movements associated with M8.1 earthquake in Solomon Islands on April 1, 2007, detected by ALOS/PALSAR

Yousuke Miyagi[(1)], Taku Ozawa[(2)], Yuichi Nishimura[(3)], and Masanobu Shimada[(1)]

[(1)]Japan Aerospace Exploration Agency / Earth Observation Research Center, Tsukuba Space Center, 2-1-1 Sengen, Tsukuba, Ibaraki 305-8505, Japan, E-mail: miyagi.yousuke@jaxa.jp, shimada.masanobu@jaxa.jp
[(2)]National Research Institute for Earth Science and Disaster Prevention, 3-1 Tennodai, Tsukuba, Ibaraki 305-0006, Japan, E-mail: taku@bosai.go.jp
[(3)]Institute of Seismology and Volcanology, Hokkaido University, N10W8 Kita-ku, Sapporo, Hokkaido 060-0810, Japan

Abstract

We describe the large M8.1 earthquake occurred in Solomon Islands on April 1, 2007, as an example of disaster monitoring and observation in remote locations by ALOS/PALSAR. Comparing PALSAR images observed before and after the earthquake, we could find some changes associated with the earthquake. We went to the Solomon Islands in the end of July and investigated the damaged area. Ground deformations were detected over a wide area using a DInSAR technique. We presume that such deformations represent co-seismic deformations caused by faulting, and try to model these observed deformations using a fault model. Results from this modeling can account for observed data well and are in good agreement with results from modeling using a teleseismic body wave.

Keywords: PALSAR, DInSAR, ground movement, earthquake, Solomon Islands

1. INTRODUCTION

The Solomon Islands is a nation composed of about 10 main islands and a thousand small islands located in the southwest Pacific Ocean. Two major plates, the Pacific and Australian plates, and two minor plates, the Solomon Sea and Woodlark plates, produce complicated tectonics in the southwest off the Solomon Islands [Tregoning et al., 1998] (Fig. 1). On April 1, 2007 (UTC), a M8.1 interplate earthquake occurred in the subduction zone between the Pacific Plate and the Australian Plate (S8.48°, E156.98°) [see the USGS web site for time of occurrence, type, magnitude, and location of the earthquake: http://earthquake.usgs.gov/eqcenter/eqinthenews/2007/us2007aqbk/]. This earthquake was accompanied by a large tsunami and caused considerable damage in the area. The Japan Aerospace Exploration Agency (JAXA) performed emergency observation using the Advanced Land Observing Satellite (ALOS) and tried to acquire information on the afflicted area as soon as possible.

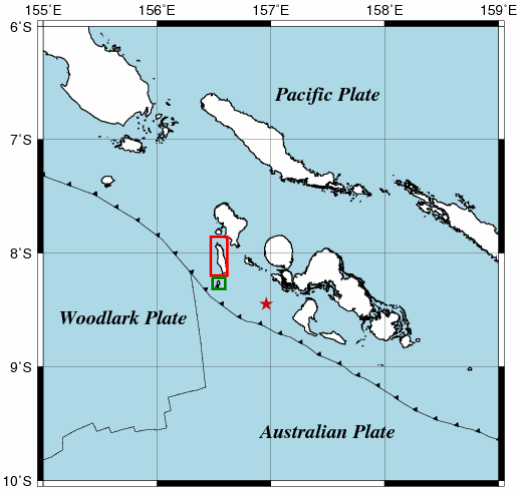

Figure 1. Study area (Solomon Islands) with plate boundary defined by PB2002 [Bird, 2003]. Red star represents the epicenter.

A remote-sensing technique has the advantage of being able to observe and monitor a disaster that has occurred in a remote location like the Solomon Islands that is difficult to access and receives few geophysical observations. The Phased Array type L-band Synthetic Aperture Rader (PALSAR) installed on ALOS is especially well-suited for these purposes in contrast to an optical sensor that often suffers from cloud coverage in the tropical region. PALSAR provides much data because it can observe the target day and night and even under cloudy conditions. Furthermore, PALSAR data can be applied in Differential Interferometric SAR (DInSAR) techniques to detect precise ground deformation. Such precise geodetic data is helpful for inferring a fault model. If it is possible, field investigation is helpful for verifying the remotely sensed data. We went to the Solomon Islands in late July 2007 and investigated the area damaged by the earthquake and tsunami.

In this paper, we compare the PALSAR images observed before and after the earthquake in Solomon Islands to detect changes associated with the earthquake

and compare the data from remote sensing with that from field investigation. We then present the observed ground deformation using the DInSAR technique and the result of fault modeling with DInSAR data.

2. SATELLITE AND FIELD DATA

Figures 2a and 2b are amplitude images of the southern part of Ranongga Island acquired before and after the earthquake. Comparing these images, we find an apparent increase of coastal land area in Fig. 2b in spite of the rising tide level. We presume that some uplift associated with the earthquake occurred in these areas, although it is difficult to assess quantitatively using just these data. Figure 3 is a picture of the area enclosed by the red circle in Fig. 2b on July 28, 2007. In the field investigation of this area, we could see evidence of a major uplift of three or more meters. Figures 4a and 4b are amplitude images of the northern part of Simbo Island acquired before and after the earthquake. In contrast to Ranongga Island, Simbo Island exhibits decreasing land area for the period. This is not clear evidence of subsidence because it may be caused by tidal changes. However, at least, there was no uplift as on the neighboring Ranongga Island.

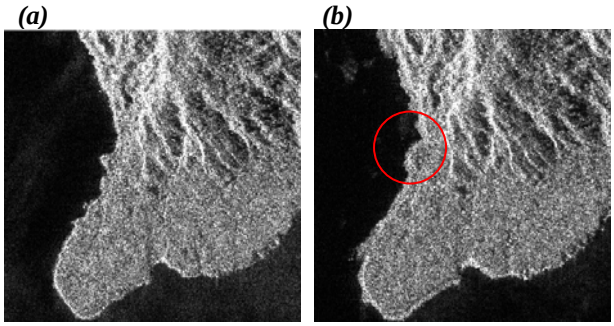

Figure 2. PALSAR amplitude images observed before (a) and after (b) the earthquake in the southern part of Ranongga Island (red rectangle in Fig. 1).

Figure 3. Huge uplift in Lale (Red circle in Fig. 2b). Author stands beside a 3 m scale in the picture.

In Tapurai, a small village located on the northern part of Simbo Island (yellow circle in Fig. 4b), almost all buildings were destroyed by a large tsunami. In contrast, there was almost no tsunami damage in Lale, a village located on the southern Ranongga Island (red circle in Fig. 2b) only 10km north of Tapurai. This suggests that the uplift occurred before the tsunami in Lale, and there was no uplift in Tapurai. There may be a boundary of uplift and subsidence between Simbo and Ranongga islands.

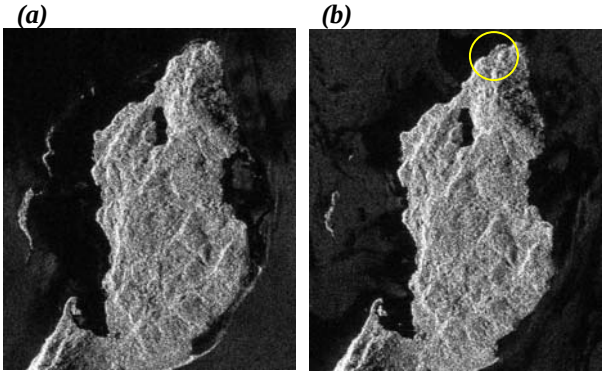

Figure 4. PALSAR amplitude images observed before (a) and after (b) the earthquake in the northern part of Simbo Island (green rectangle in Fig. 1).

3. DIFFERENTIAL INSAR AND FAULT MODEL

Although we can see that something occurred or the pattern of some phenomena by comparing amplitude images, we can't understand what it was or how great it was. However, ground deformation derived from DInSAR processing is quite precise geodetic information and can be used for quantitative discussion. Figure 5 presents interferograms in the study area, composed of three consecutive paths (Paths: 343 to 345). The color fringe in Fig. 5 represents the ground deformation in a slant range component, which can be interpreted as being induced by a reverse dip-slip in the supposed seismic fault.

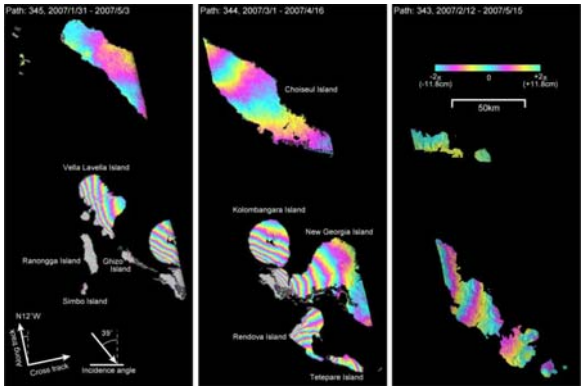

Figure 5. Interferograms generated by DInSAR technique showing ground deformation associated with the earthquake.

We next tried to model the observed geodetic information by fault modeling. In this modeling, we first set locations and a strike direction of the fault area so as to include the plate boundary defined by PB2002 [Bird, 2003]. We assume the size of the fault area 360km long and 150km wide, divide it into sub-faults of 24×10, and estimate the slip vector for each sub-fault. A dip angle of the fault is determined so as to minimize the ABIC. To avoid the problem of not knowing the absolute displacements and the relationship of displacements among islands, we set biased displacements for each island. An orbit tuning is not performed in the DInSAR processing, so there is a possibility that a non-crustal deformation component remains in each interferogram. Because the remnant of the orbital component can be considered as a uniformly inclined plane due to a precise determination of the orbit information of ALOS satellite, we define non-crustal deformation component as a plane and estimate them for each orbital path.

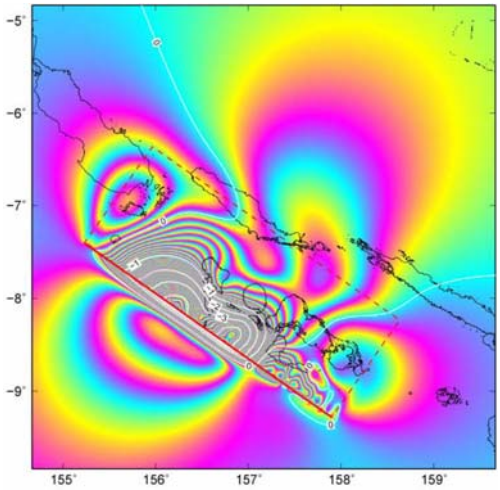

Figure 6. Calculated interferogram using best-fit parameters. Color fringe represents displacement in slant range component.

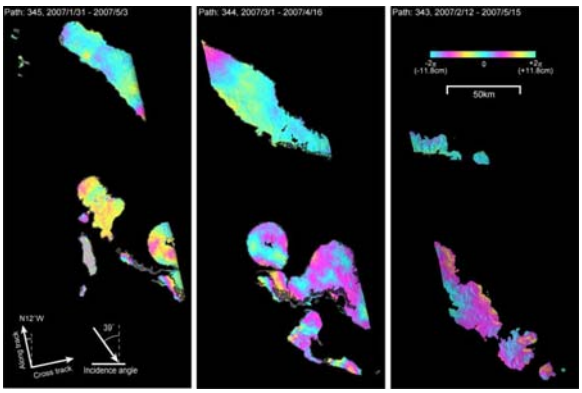

Figure 7. Residuals between observed and calculated interferograms. The small residual indicates good agreement between both interferograms.

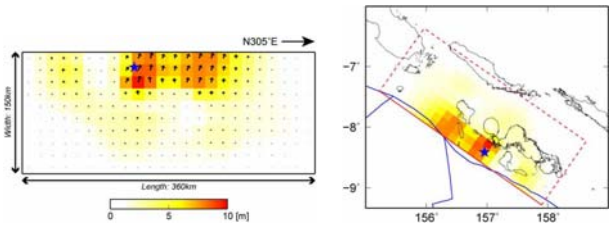

Figure 8. Slip distribution on the supposed fault plane.

Figure 6 depicts the calculated interferogram using best fit parameters, and Fig. 7 illustrates the residuals between observed and calculated interferograms for each path. The model well explains the observed data and the pattern of slip distribution (Fig. 8), which has a two-eyed large slip area around the hypocenter and northwest of it, is similar to that deduced from the teleseismic body wave data [Yamanaka, 2007].

4. CONCLUSIONS

ALOS/PALSAR could acquire favorable data for understanding phenomena associated with the large earthquake in the Solomon Islands. Comparison of amplitude images before and after the earthquake revealed that something had occurred and this was confirmed by the field investigation. Satellite and the field investigation data revealed a major uplift in Ranongga Island and small uplift or subsidence in Simbo Island and this agreed with the difference in tsunami damage on the two islands. Significant ground deformation was detected over the wide area using the DInSAR technique. From these geodetic data, we inferred a fault model and slip distribution for the earthquake. Although it is a preliminary result, the model well explains the observed deformation, and exhibits good agreement with that inferred from the teleseismic data, in which they had a two-eyed large slip area.

5. ACKNOWLEDGEMENT

Copyrights of ALOS/PALSAR data used in this study are all reserved by JAXA and METI.

REFERENCES

[1] Tregoning, P., et al., Estimation of current plate motions in Papua New Guinea from Global Positioning System observations, J. Geophys. Res., 103, pp.12,181-12,203, 1998.

[2] Bird, P., An updated digital model of plate boundaries, G. Geophys. Geo., Vol. 4, No. 3, 1027, doi:10.1029/2001GC000252, 2003.

[3] Yamanaka, Y., NGY seismology note on the web: http://www.seis.nagoya-u.ac.jp/sanchu/Seismo_Note/2007/RSVD1.html, 2007.